

# PRELIMINARY RESULTS TO SUPPORT EVIDENCE OF THERMOSPHERIC CONTRACTION

**Arrun Saunders, Graham G. Swinerd, Hugh G. Lewis**

*School of Engineering Sciences*

*University of Southampton, Highfield, Southampton, SO17 1BJ, UK,*

## ABSTRACT

Atmospheric density has an important influence in predicting the positions of satellites in low Earth orbit. For long-term predictions of satellite ephemerides, any future density trend in the thermosphere would be a valuable input, not only to satellite operators, but also to studies of the future low Earth orbit environment in terms of space debris. A secular thermospheric density trend has not yet been definitively proven but predictions by Roble and Ramesh [1], along with evidence by Keating *et al.* [2] and Emmert *et al.* [3 & 4], strongly suggest the existence of such a phenomenon. With the ultimate goal of deriving a long-term empirical model of thermospheric cooling and contraction, the primary focus of this paper is to present preliminary results obtained to support the existing evidence for such a thermospheric contraction. The results from four satellites over 30 years indicate a thermospheric mass density decline of  $-4.1 \pm 0.7$  % per decade above an altitude of approximately 355 km.

## 1. INTRODUCTION

There are many ways of determining atmospheric density, but inferring thermospheric density from satellite drag data is a relatively cost-effective way of gathering in-situ measurements. Given an initial satellite orbit, one approach is to use an orbital propagator to predict the satellite's state at some time ahead and then to compare that state with Two-Line Element (TLE) data at the same epoch. The change in the semi-major axis due to drag is used as a proxy for indicating thermospheric density changes. This is the approach adopted in our new work, using a dedicated, orbital propagator that includes perturbations due to atmospheric drag, gravitational anomalies, luni-solar gravity and solar radiation pressure effects. The method used to derive precise estimates of the ballistic coefficient of each satellite for use in the propagator is outlined, as this information is not contained explicitly in the TLE sets. In validation of the orbital propagator used in this study, Saunders *et al.* [5] ran simulations to predict satellite re-entry dates with satisfactory results. Now, historical satellite data between the years 1970 and 2000 have been used to infer a secular thermospheric density change. The NRLMSISE-00 (Naval Research Laboratory's Mass Spectrometry and Incoherent Scatter Radar up to the Exobase, released in the year 2000) empirical standard atmospheric model is used to predict thermospheric densities in the orbital propagator. More recent atmospheric models have not been used due to their use of atmospheric state indices (e.g. the Disturbance Storm Time index utilized by the latest Jacchia-Bowman models) which are not available for the complete historical time period.

During the last 30 years there has been a lively debate on whether atmospheric changes caused by human activity will have significant long-term effects on the structure of the atmosphere and the general climate of the Earth. Temperatures in the mesosphere and thermosphere were predicted to cool by 10 K and 50 K respectively for a doubling in the CO<sub>2</sub> and CH<sub>4</sub> atmospheric concentrations [6]. This cooling would collapse the density structure and result in an overall contraction of the atmosphere. Current forecasts predict a doubling in the CO<sub>2</sub> mixing ratios by the end of the 21st century [7]. The first study in the field of thermospheric contraction due to anthropogenic activities, specifically dealing with declining thermospheric densities, was made by Keating *et al.* [2] in 2000. This study used the long-term orbital decay of five satellites with perigee altitudes averaging around 350 km. The results provide evidence of an average of  $-9.8 \pm 2.5$  % in thermospheric densities between the years 1976 and 1996. The method incorporated an analytical approach given by King-Hele [8] using orbital elements given in TLE sets. However, using the orbital parameters directly from the TLE sets gives inaccurate results, due to the removal of some periodic orbital variations.

Using 27 long-lived near-Earth space objects, Emmert *et al.* [3] used a more accurate method of predicting thermospheric densities using TLE data [9], to derive trends in upper thermospheric density. The data covered all levels of solar variability spanning the time period of 1966-2001. The results indicated a density trend of -2 % per decade at 200 km altitude, decreasing to -5 % per decade at 700 km. This supports the idea of a 'pancake effect' occurring from cooling mechanisms lower in the atmosphere. Later in 2008, Emmert *et al.* [4] performed a similar study, this time using 5000 orbiting objects. The results at 400 km showed an overall density trend of  $-2.68 \pm 0.49$  % per decade and trends of -5 and -2 % per decade at solar minimum and maximum, respectively.

The four satellites used in the current study were a subset of the five used by Keating *et al.* [2], which had the USSN (United States Space Surveillance Network) numbers 00060, 00614, 02389 and 04330. This overlap allowed the results from this study to be compared with those of Keating *et al.* The historical TLE data for these satellites were obtained from the online database Space Track [10].

## 2. THE ORBITAL PROPAGATOR

An Earth orbital propagator for thermospheric analysis (named AETHER) was written in the programming language C++ to predict the orbital evolution of the satellites under investigation. AETHER works by taking the initial conditions of a satellite, and then propagating its orbit numerically using a 7<sup>th</sup> order Runge-Kutta-Fehlberg method. Spatially it requires a Cartesian state vector of the satellite's position and velocity relative to the centre of the Earth. Temporally it uses the year and the decimal day of the year of the satellite's TLE epoch. Finally a ballistic parameter of the satellite, which will be discussed in greater detail later, is required to estimate the atmospheric drag. As the source of satellite initial conditions given by TLEs are in the form of classical orbital elements, a conversion to a Cartesian state vector is required. This conversion tool came in the form of the freely available Simplified General Perturbations (SGP4) analytical propagator [11]. The SGP4 propagator is the tool by which the TLE sets are initially produced, and due to the unique way in which periodic orbital variations are removed, the conversion back to a Cartesian state vector needs to be performed in an exactly reversed manner [11]. The output coordinate system of the SGP4 Cartesian vectors uses the True Equator Mean Equinox of Epoch (TEME). The AETHER orbital propagator used for this study was written to use the same system.

Currently there are four sources of perturbation that make up the acceleration model for the satellite propagation in AETHER, these are: gravity anomalies using the Joint Gravity Model (JGM3) [12] to order and degree 18, atmospheric drag using the NRLMSISE-00 empirical atmospheric model [13] for density predictions (further the atmosphere is assumed to be co-rotating with the Earth), luni-solar gravity effects and perturbations from solar radiation pressure.

The validation of AETHER took the form of re-entry predictions of three satellites, discussed by Saunders *et al.* [5]. These satellites, with USSN numbers 10973, 20967 and 26873 decayed in March 2007, January 2007 and December 2005 respectively. Using TLE data up to 15 days prior to the known decay date, the satellite ephemerides were input to AETHER and demise re-entry prediction dates were obtained. The process of validating the AETHER software was aided by the comparison of the actual and predicted re-entry dates. The results shown in Fig. 1.

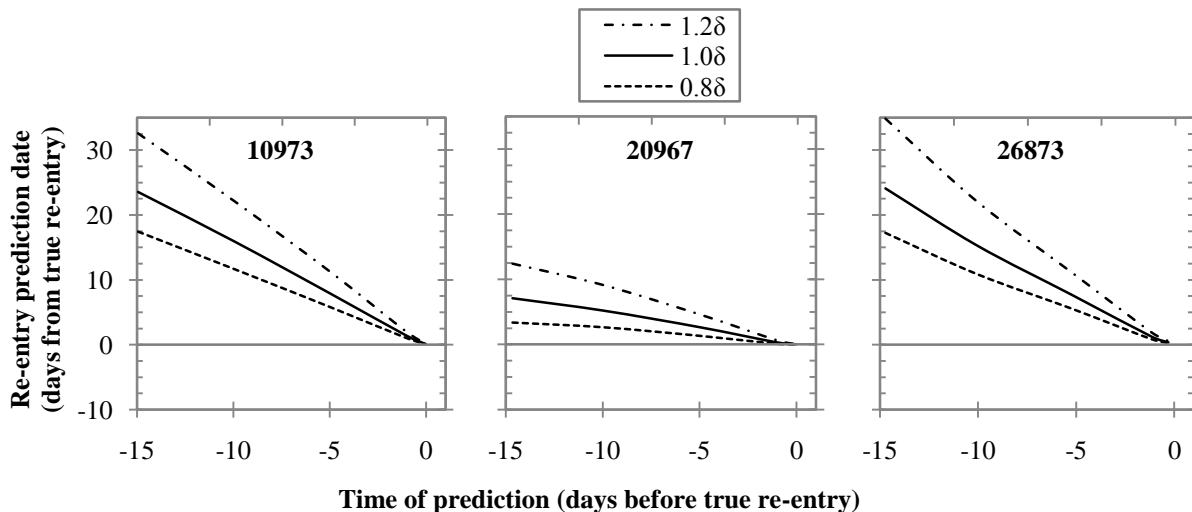


Fig. 1. Re-entry prediction dates for satellites 10973, 20967 and 26873 produced by AETHER. Three values of ballistic coefficient  $\delta$  were used due to the variability of a satellite's projected surface area.

A drawback of this study was the use of the  $B^*$  parameter given directly in the TLE data, from which a ballistic coefficient was estimated. However, as the  $B^*$  parameter is used as a fitting parameter when the TLE sets are originally created [14], using it to estimate a satellite's ballistic coefficient can provide erroneous values. This is the main source of error shown in the results presented in Fig. 1. However, satisfactory measure of validation of AETHER was achieved. The conclusion was that AETHER could accurately predict a satellite's future ephemerides as long as better estimates of its ballistic coefficients were made. The reader is referred to Saunders *et al.* [5] for more detail.

### 3. BALLISTIC COEFFICIENT

An empirical method is developed to improve the estimates of satellite ballistic coefficients used in AETHER, in conjunction with the historical TLE data. This method involves taking a subset of a satellite's historical TLE database from which a ballistic coefficient is estimated. The semi-major axes  $a_{1,2}$  of two consecutive TLE sets (TLE<sub>1</sub> and TLE<sub>2</sub>), are estimated using

$$a_{1,2} = \frac{\mu r_{1,2}}{2\mu - v_{1,2}^2 r_{1,2}}, \quad (1)$$

where  $\mu$  is the Earth's gravitational constant (398600.4415 km<sup>3</sup>/s<sup>2</sup>),  $r$  is the satellite's distance from the centre of the Earth and  $v$  is the satellite's velocity in the TEME coordinate system. The positions and velocities are obtained from the state vectors, produced from the TLE sets via the SGP4 propagator. Having obtained estimates of the semi-major axes at the TLE<sub>1</sub> and TLE<sub>2</sub> epochs, the ephemeris of TLE<sub>1</sub> is used as the initial condition for propagation using AETHER. In addition, an initial estimate of the ballistic coefficient is given by the B\* parameter contained within the TLE data. After numerical propagation of the satellite from the epoch of TLE<sub>1</sub> to that of TLE<sub>2</sub>, a new semi-major axis  $a_2^*$  is estimated from the resulting state vector. The difference between  $a_2$  and  $a_2^*$  is calculated, and the ballistic coefficient is adjusted, using the Secant method,

$$\delta_n = \delta_{n-1} - \frac{\Delta a(\delta_{n-1}) \cdot \{\delta_{n-1} - \delta_{n-2}\}}{\Delta a(\delta_{n-1}) - \Delta a(\delta_{n-2})}, \quad (2)$$

where  $\Delta a(\dots)$  denotes the difference between  $a_2$  and  $a_2^*$  using the respective iterative ballistic coefficient estimate,  $\delta_n$ . The propagation is then restarted from the initial conditions of TLE<sub>1</sub>. This process is repeated until the difference between  $a_2$  and  $a_2^*$  reaches a sufficiently small value, thereby giving a more accurate method of estimating the ballistic coefficient. To validate this method, the study of satellite re-entry by Saunders *et al.* [5] described earlier was repeated with updated values of ballistic coefficients. 200 TLE sets for each satellite prior to the initial prediction date (-15 days) were used, with the results shown below in Fig. 2.

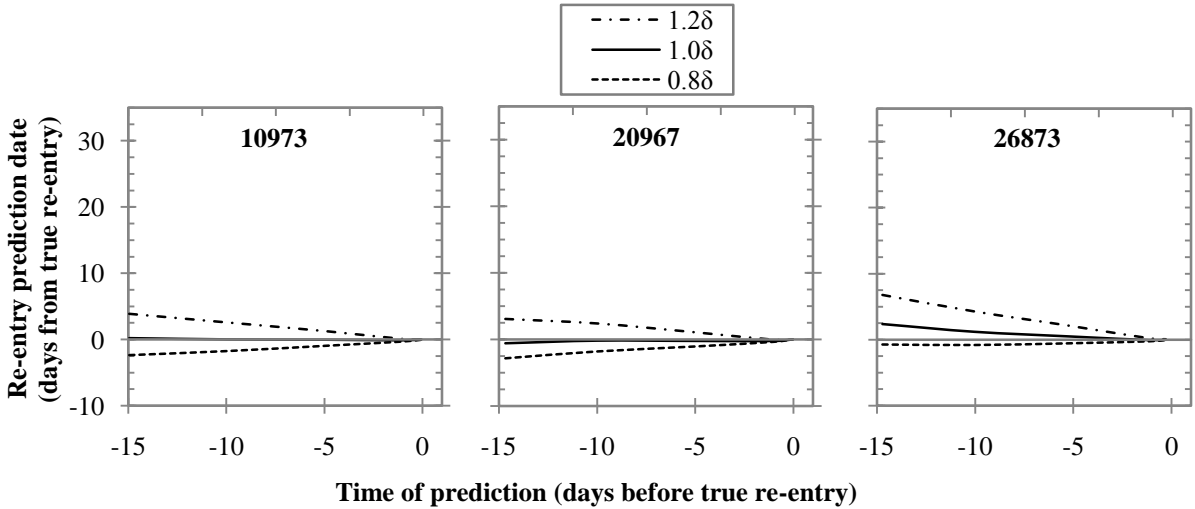


Fig. 2. The re-entry prediction dates for satellites 10973, 20967 and 26873 produced by AETHER using updated estimates of ballistic coefficient.

From Fig. 2, the predictions of the satellite's re-entry dates were significantly improved from those shown in Fig. 1. This reinforced confidence in the AETHER software, and also indicated that accurate values of the ballistic coefficient can be obtained using the method described above.

Approximately 950 TLE sets from the years 1999 and 2000 were used to estimate ballistic coefficients for each of the four satellites used in this study. It is essential that the time period of historical TLE data from which a ballistic coefficient estimate is made, is significantly smaller than the period from which a secular mass density trend is derived. This is because estimating the ballistic coefficient in this way requires the use of a reference historical period to which a secular density trend is compared. If this reference period is similar in duration to the entire historical data then any secular density trends may be averaged out during the estimation of the ballistic coefficient.

With reliable estimates of ballistic coefficients, and an appropriate span of historical TLE sets, all the required data was available to attempt a preliminary analysis of thermospheric contraction trends.

#### 4. METHODOLOGY

Previous studies investigating secular thermospheric mass density trends have used a method whereby an absolute measurement of mass density is derived, and associated with a specific altitude [3 & 4]. This derived density is then compared to a density predicted by an empirical atmospheric model, such as the NRLMSISE-00. The method presented here to determine a mass density trend does not involve predicting a mass density at a specific location or altitude. Here, the changes caused by atmospheric drag, and therefore indicating thermospheric density, to a satellite's orbit are used to infer thermospheric density variations. This is where the distinct objectives of thermospheric mass density prediction and thermospheric mass density trends diverge. In this study it is shown that to derive a secular trend in global average thermospheric mass density, it is not necessary to explicitly determine absolute density values. A different approach can be taken by analysing the changes in satellite orbits caused by thermospheric mass density. The orbital parameter used in this study to determine thermospheric density trends, is the change in semi-major axis. The method compares the change in semi-major axis derived directly from the TLE data, to that predicted by AETHER.

Ultimately we will only need to know the change in semi-major axis to determined density trends. However, to begin with, let us falsely assume that in order to determine a secular mass density trend, explicit thermospheric density estimates need to be made. Therefore, a comparison between the observational data of the TLEs, and that from numerical predictions, using AETHER, needs to be made. The comparison parameter  $\zeta$  is defined by

$$\zeta = \frac{\rho}{\rho^*}. \quad (3)$$

Here  $\rho$  denotes the density derived from the TLEs, and  $\rho^*$  is the density derived using AETHER. From King-Hele [8] the density at a point on an orbit can be defined by

$$\rho = \frac{-\mu\dot{a}}{a^2 v^2 \delta}, \quad (4)$$

where  $\dot{a}$  is the rate of change of the semi-major axis with respect to time and the other variables having their usual meanings. Now let us assume that the parameters in (4) refer to a satellite orbit at an epoch of say, TLE<sub>1</sub>. All the parameters are therefore known except the rate of change of the semi-major axis  $\dot{a}$ , which can be calculated by

$$\dot{a} = \frac{a_2 - a_1}{\Delta t}, \quad (5)$$

where  $\Delta t$  is the time difference between TLE<sub>1</sub> and TLE<sub>2</sub> and  $a_1$  and  $a_2$  are their respective semi-major axes. Here,  $\dot{a}$  has been derived using only the observational data of the TLEs. The rate of change for the numerically derived data is then given by

$$\dot{a}^* = \frac{a_2^* - a_1}{\Delta t}, \quad (6)$$

where  $a_1$  and  $\Delta t$  are the same as in (5), but  $a_2^*$  has now been determined from the numerically propagated orbit using AETHER. Using (4) a density derived from numerical propagation can be given by

$$\rho^* = \frac{-\mu\dot{a}^*}{a^2 v^2 \delta}. \quad (7)$$

Combining (4)-(7), inserting in (3) and simplifying gives

$$\zeta = \frac{a_2 - a_1}{a_2^* - a_1} = \frac{\Delta a}{\Delta a^*}. \quad (8)$$

The most significant orbit perturbation that affects the semi-major axis in a secular manner is drag. Other perturbations affect the semi-major axis, but most average out over an orbit cycle due to their periodic character. Some perturbations, however, do cause a secular variation in the semi-major axis, such as the combination of

solar radiation pressure and gravity anomalies as a satellite passes in and out of Earth's shadow. However, these variations are small compared to those produced by drag, and are assumed to be negligible. Therefore, from the historical TLE data the change in semi-major axis can be obtained in two ways. One way is to use the mean mean motion, given directly in the TLE sets, to estimate a semi-major axis. Another approach is to use (1) and the state vectors given via the SGP4 propagator. Fig. 3 shows the variation of semi-major axis derived using the two methods from 10 years of TLE sets for satellite 02389.

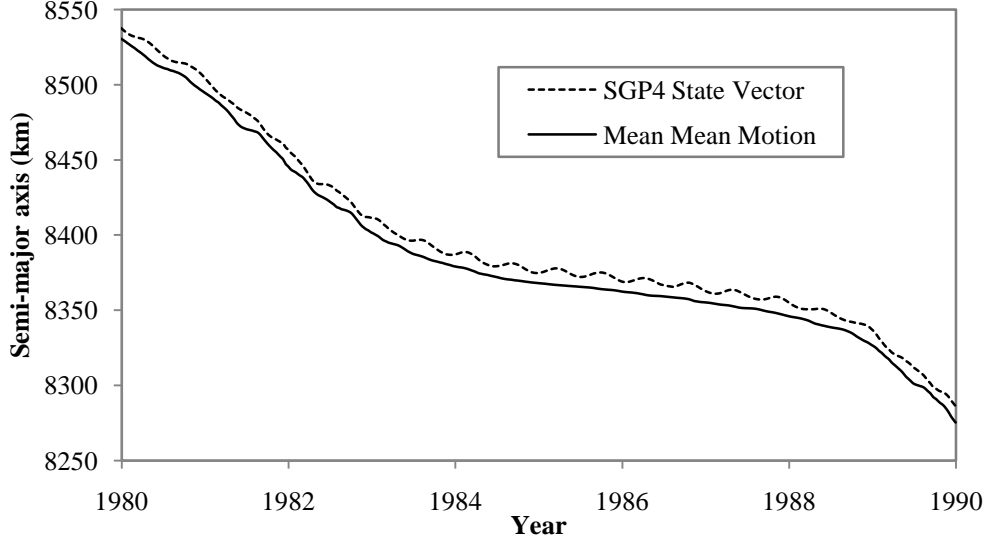


Fig. 3. A 10-year sample of the variation in semi-major axis for satellite 02389, derived using the SGP4 state vectors and the mean mean motion given in the TLE sets.

From Fig. 3 the semi-major axes derived in the two different ways follow the same trend. As the parameter required by the current analysis is the change in semi-major axis, and not the specific value, the method using the mean mean motion provides the smoothest data. Therefore, this is the method used to calculate  $\Delta a$  given in (8).

To derive  $\Delta a^*$  from (8), AETHER calculates only the changes in the semi-major axis due to drag. It can be shown that only forces with tangential components to the satellite's velocity vector affect the semi-major axis [8],

$$\dot{a} = \frac{2a^2 v}{\mu} f_T, \quad (9)$$

where  $f_T$  denotes the force per unit mass parallel to the satellite's velocity vector and  $a$  is the instantaneous semi-major axis calculated from the osculating state vector.  $f_T$  is thus the sum of accelerations from all perturbations parallel to the satellite's velocity vector. Therefore, the rate of change of semi-major axis due only to drag is,

$$\dot{a}_{drag} = \frac{2a^2 v}{\mu} \dot{r}_{drag}, \quad (10)$$

where  $\dot{r}_{drag}$  is the acceleration due to drag, calculated explicitly during the propagation in AETHER. Finally, the total change in semi-major axis due to drag predicted by AETHER is given by

$$\Delta a^* = \int_{TLE1}^{TLE2} \dot{a}_{drag} dt. \quad (11)$$

The density variations in the atmosphere detected via the changes in the semi-major axes are associated with a specific region. This region is bounded by the lower and upper altitudes of the satellite's orbit, as shown below in Fig. 4. As the planned number of satellites used to analyse the historical TLE catalogue is large, the regions of the atmosphere analysed will form an altitude dependent model of secular thermospheric mass density trends.

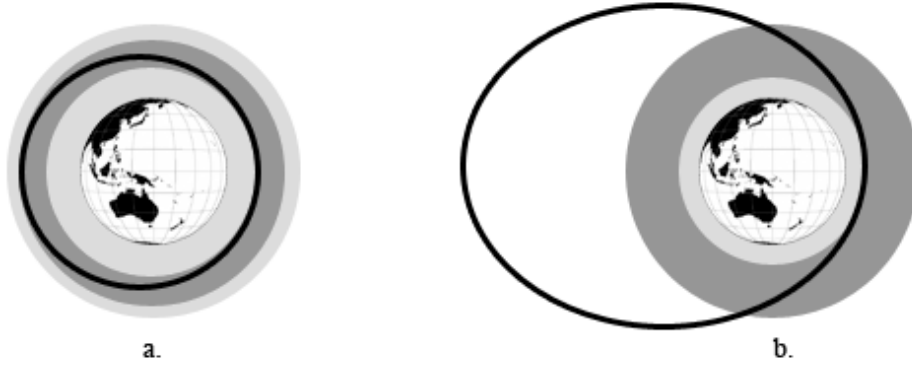


Fig. 4. Altitude regions of the Earth's atmosphere analysed by using the method presented in this study are denoted by the dark grey areas, with the whole atmosphere represented by both grey areas. Two examples of satellite orbits are shown by the black ellipses. Case a: Altitude varies slightly covering a small band of the atmosphere. Case b: Altitude varies greatly, with the satellite effectively exiting the atmosphere.

## 5. RESULTS

The use of the historical TLE data covering the years 1970 to 2000 and the application of the method described above to the four satellites (00060, 00614, 02389 and 04330), yields negative secular thermospheric mass density trends. Table 1 presents the results for the individual satellites.

Table 1. Satellite characteristics and their respective density trends ( $\zeta$ ) presented in this study.

Satellite Number	Satellite Name	Perigee Height (km)	Apogee Height (km)	$\zeta$ (1976-1996 % per 20-years)	$\zeta$ (1970-2000 % per decade)	Estimated Ballistic Coefficient ( $\text{km}^2/\text{kg}$ )
00060	Explorer 8	418-390	2142-1202	-7.87	-4.15	$2.742 \cdot 10^{-8}$
00614	Hitchhiker 1	337-324	3884-2289	-9.28	-3.95	$1.513 \cdot 10^{-8}$
02389	OV3-3	355-350	4324-2977	-9.71	-4.78	$1.839 \cdot 10^{-8}$
04330	Oshumi	350-315	5140-1912	-3.66	-3.36	$2.870 \cdot 10^{-8}$
All	-	418-315	5140-1202	$-7.5 \pm 3.0$	$-4.1 \pm 0.7$	-

As the satellites used in this study have relatively high apogee altitudes, their orbital geometry resembles Case b, in Fig. 4. Therefore by averaging the perigee altitudes of the four satellites, a statement can be made about the historical thermospheric mass density evolution above altitudes of approximately 355 km. By collating all the results for the individual satellites and applying a linear least squares regression, a secular decline in thermospheric mass density was determined as shown in Fig. 5. Therefore, since 1970 and above an altitude of 355 km, thermospheric mass density has appeared to reduce by an average rate of  $-4.1 \pm 0.7$  % per decade. The error margin stated here is calculated using the maximum and minimum trend values given by satellites 02389 and 04330 respectively. This study only uses data from four satellites. It is planned to use many more in order to reduce the noise, as seen in Fig. 5, and increase the strength of any secular signal.

During the historical time period of 1970 to 2000, more than two solar cycles occurred. Therefore the data presented here covers all levels of solar variability. It was shown by Emmert *et al.* [3] that thermospheric density variations appeared dependent on solar activity, and therefore this will be investigated further. By applying a 300-day moving average to the trend data and plotting the result against solar flux a rough correlation can be seen in Fig. 6.

For each satellite, it took an average of 7.5 hours to complete the 30-year analysis, using a 2.4 GHz processor and an integration step size of 20 seconds. Previous analysis suggested a 2 second integration step was required [15]. However, by investigating the sensitivity of the semi-major axes estimates, a 20 second integration step size was deemed sufficient. Optimisations in AETHER to reduce the computational effort will most likely take the form of reducing the degree and order of the Earth's gravitational model used in the acceleration model, as these calculations require the most computational effort.

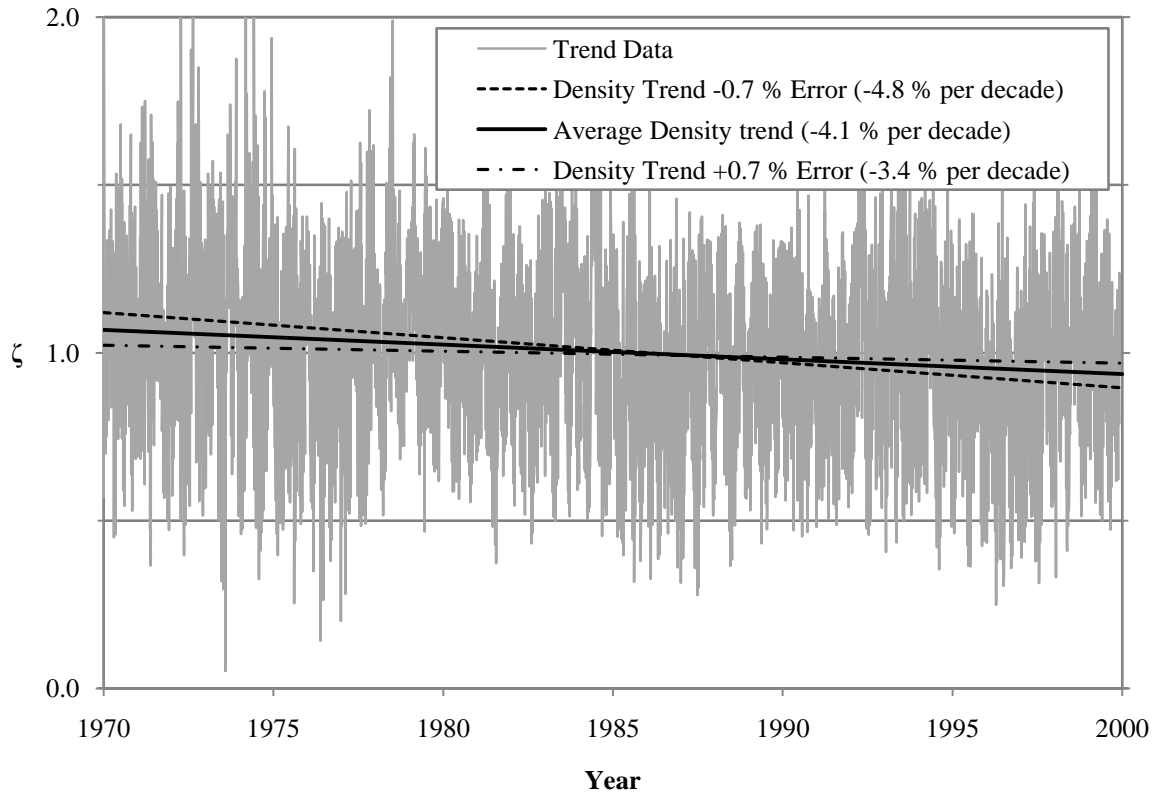


Fig. 5. The collated results showing a secular thermospheric mass density trend over the years 1970 to 2000.

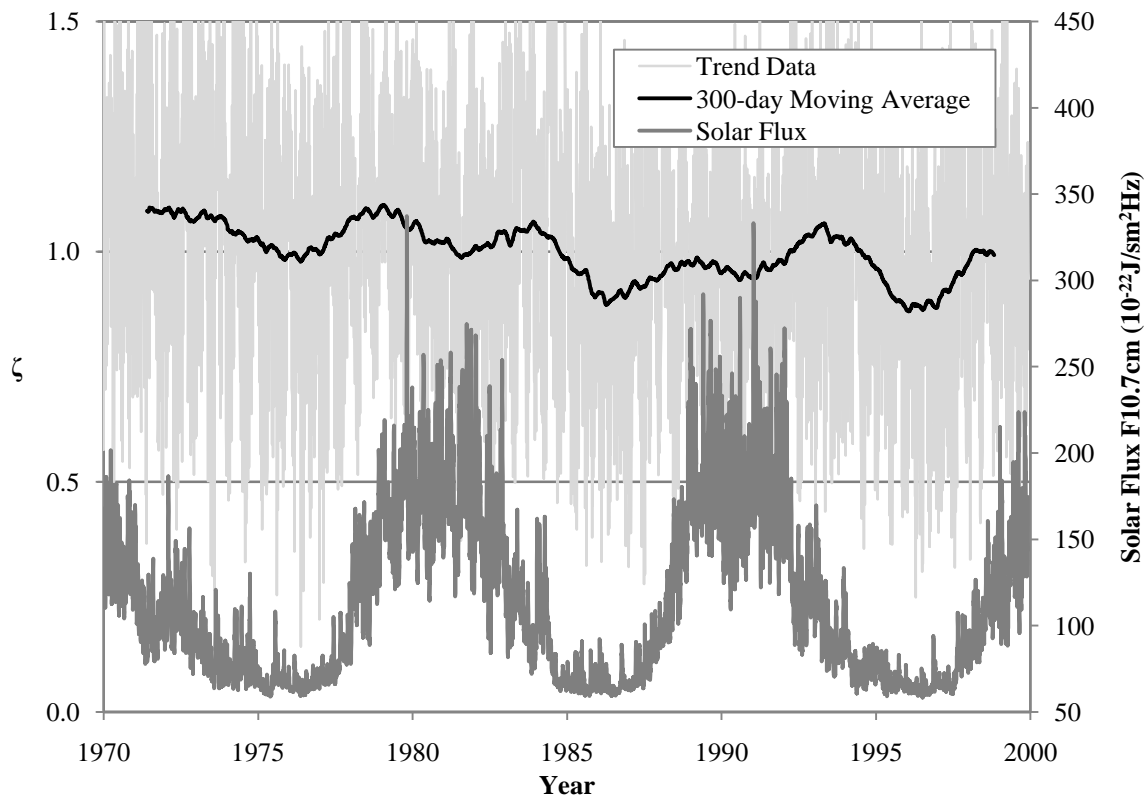


Fig. 6. A 300-day moving average of the trend data shown with the corresponding F10.7cm solar flux.

## 6. CONCLUSION

This study is very preliminary in nature, but has tentatively confirmed evidence supporting the existence of a secular thermospheric mass density decline. The objective of this paper, to present preliminary results by exercising the method derived to confirm a long-term empirical model of thermospheric contraction, has been achieved with satisfactory results. Although the results are based on a small number of satellites, they nevertheless provide a good grounding in the use of the software AETHER and of the derivation techniques used to determine a secular thermospheric density change.

A new method to derive thermospheric density trends has also been presented. By calculating the change in semi-major axes due to drag from two different data sources, via (8), relative density trends can be derived without determining absolute density values.

Comparison of the results from this study with those of Keating *et al.* [2] shows an agreement of a secular decline in thermospheric mass density. The magnitudes of the density trends were also similar. The study by Keating *et al.* gave a value of  $-9.8 \pm 2.5$  % over the 20-year period of 1976 to 1996 compared to that derived in this study of  $-7.5 \pm 3.0$  % over the same historical time period. The more detailed and robust study by Emmert *et al.* [4] derived values of  $-2.68 \pm 0.49$  % per decade, whereas this study yielded the trend of  $-4.1 \pm 0.7$  % per decade. The next step is therefore to perform the analysis using a much larger satellite population.

During the analysis, it became clear that various optimisations in the software AETHER will need to be made, in order to efficiently apply these processes to a large number of satellites. However, now this initial study has been completed, it can be used as a datum to optimise aspects of the AETHER software in order to perform more efficiently.

## 7. REFERENCES

1. Roble, R. G. and Ramesh, D. S., Cooling Mechanisms of the Planetary Thermospheres: The Key Role of O Atom Vibrational Excitation of CO<sub>2</sub> and NO, *CHEMPHYSICHEM* 2002, 3, 841-843 1 WILEY-VCH Verlag GmbH & Co. KGaA, Weinheim, 2002.
2. Keating, G. M. *et al.*, Evidence of long-term global decline in the Earth's thermospheric densities apparently related to anthropogenic effects, *Geophys. Res. Lett.*, 27, 1523-1526, 2000.
3. Emmert, J. T. *et al.*, Global change in the thermosphere: Compelling evidence of a secular decrease in density, *J. Geophys. Res.*, 109, A02301, doi:10.1029/2003JA010176, 2004.
4. Emmert, J. T. *et al.*, Thermospheric global average trends, 1967-2007, derived from orbits of 5000 near-Earth objects, *J. Geophys. Res.*, 35, L05101, doi:10.1029/2007GL032809, 2008.
5. Saunders, A. *et al.*, A New Tool for Satellite Re-entry Predictions, 5th European Conference of Space Debris, Darmstadt, Germany, March-April, 2009.
6. Roble, R. G. and Dickinson, R. E., How will changes in carbon dioxide and methane modify the mean structure of the mesosphere and thermosphere?, *J. Geophys. Res.*, 16, No. 12, 1441-1444, 1989.
7. Brasseur G. and Hitchman, M., Stratospheric response to trace gas perturbations: Changes in ozone and temperature distributions, *Science*, 240, 634-636, 1988.
8. King-Hele, D., *Satellite Orbits in an Atmosphere: Theory and Applications*, Blakie, Glasgow, 1987.
9. Picone, J. M., *et al.*, Thermospheric densities derived from spacecraft orbits: Accurate processing of two-line element sets, *J. Geophys. Res.*, 110, A03301, doi:10.1029/2004JA010585, 2005.
10. Space-Track.org, *Space Track: The source for space surveillance data*, www.space-track.org, 2004.
11. Hoots, F. R. and Roehrich, R. L., Models for propagation of NORAD element sets, *Spacetrack Rep.* 3, 87 pp., Off. of Astrodyn., Aerospace Defense Cent., U. S., Peterson AFB, Colorado, 1980.
12. Tapley, B. D., *et al.*, The Joint Gravity Model 3, *J. Geophys. Res.*, 101(B12), 28,029- 28,049, 1996.
13. Picone, J. M., *et al.*, NRLMSISE-00 empirical model of the atmosphere: Statistical comparisons and scientific issues, *J. Geophys. Res.*, 107, No. A12, 1468, doi:10.1029/2002JA009430, 2002.
14. Vallado, D. A., *Fundamentals of Astrodynamics and Applications*, Hawthorne CA: Microcosm Press, New York NY: Springer, 1997.
15. Saunders, A., *Nine Month Report, An Empirical Model Of Long-Term Thermospheric Cooling And Contraction*, University of Southampton, School of Engineering Sciences, UK, 2008.